RSC Advances

ROYAL SOCIETY OF CHEMISTRY

www.rsc.org/advances

Electrosynthesis and electrochromic properties of poly(amide-triarylamine)s containing triptycene units†

Sheng-Huei Hsiao* and Yu-Ting Chiu

Department of Chemical Engineering and Biotechnology, National Taipei University of Technology, Taipei 10608, Taiwan. E-mail: shhsiao@ntut.edu.tw

† Electronic supplementary information (ESI) available: See DOI: 10.1039/…

(Abstract)

Four bis(amide-triarylamine) derivatives featuring a triptycene as an interior core and terminal electroactive triphenylamine (TPA) or *N*-phenylcarbazole (NPC) groups were prepared by the condensation reactions from 1,4-bis(4-aminophenoxy)triptycene with 4-carboxytriphenylamine and *N*-(4-carboxyphenyl)carbazole, respectively, and from 1,4-bis(4-carboxyphenoxy)triptycene with 4-aminotriphenylamine and *N*-(4-aminophenyl)carbazole, respectively. The electrochemistry and electropolymerization of these bis(amide-triarylamine) derivatives were investigated. The stability of the oxidized forms of the bis(amide-triarylamine)s is affected by the orientation of amide linkage and the structure of terminal triarylamine unit. Two of the bis(amide-triarylamine)s could be electropolymerized into robust films on the electrode surface in an electrolyte solution. The electrogenerated polymer films exhibited reversible electrochemical oxidation processes and strong color changes upon electro-oxidation, which can be switched by potential modulation. The electrochromic properties of the films were evaluated by the spectroelectrochemical and electrochromic switching studies. The TPA-based film showed better electrochromic performance than the NPC-based one.

1. Introduction

Electrochromism is defined as a reversible and visible change in the transmittance and/or reflectance of a material as the result of electrochemical oxidation or reduction.[1] This functionality is of great interest for numerous applications, such as optical switching devices, color displays, smart windows, sensors, memory elements, and camouflage materials.[2] Examples of commercially available electrochromic technology includes the Boeing 787 Dreamliner dimmable windows manufactured by Gentex.[3] The property of electrochromism is not unique to conducting polymers, but is found in a variety of organic and inorganic materials.[4] Earlier effort has been put forth on electrochromic devices based on inorganic

electrochromic systems such as tungsten oxide (WO_3) and nickel oxide (NiO or Ni_2O_3).[5] π-Conjugated organic polymers present improved processability and better color tuning ability than their inorganic and molecular counterparts.[6] Considerable effort in the Reynolds research group has been focused on the understanding and the tailoring of electrochromic properties in conjugated polymers such as poly(3,4-alkylenedioxythiophene)s (PEDOT)[7] and poly(3,4-alkylenedioxypyrrole)s (PEDOP).[8] Many other conjugated polymer systems exhibiting attractive electrochromic performance have also been explored by other research teams.[9] Electrochromic materials made from π-conjugated polymers have been gaining in popularity because they combine several advantages such as fast response time, high optical contrast ratios, color variability, and good long-term stability as well as mechanical deformability. Conjugated polymers can be synthesized by either chemical or electrochemical polymerization. Compared with the chemical routes, electrochemical polymerization can obtain conjugated polymer films on conductive substrates directly. This not only enlarges the scope of candidate polymers, but also avoids the procedure of the film coating.

Triarylamine and carbazole derivatives are well-known for their electroactive and photoactive properties that may find optoelectronic applications as photoconductors, hole-transporters, and light-emitters.[10] As a class of promising electrochromic materials, triarylamine-containing high-performance polymers such as aromatic polyamides and polyimides have various useful properties such as easily forming relatively stable polarons (radical cations), high carrier mobility, high thermal stability, and good mechanical properties.[11] In general, this kind of electrochromic polymers have been prepared by conventional polycondensation technique based on oligoaniline or triarylamine-containing diamine or dicarboxylic acid monomers.[12-14] On the other hand, electroactive and electrochromic polymer films with triarylamine units could be directly fabricated on the electrode surface via triphenylamine or carbazole-based electrochemical oxidative coupling reactions from various triarylamine-terminated electropolymerizable monomors in an electrolyte solution.[15]

Triptycene is a rigid molecular unit with three blades each composed of a benzene ring. The use of triptycene moiety as a rigid and shape-persistent component is a method to introduce molecular-scale free volume into a polymer film. Polymers with high triptycene content were reported to be interesting low-*k* dielectric materials due to the high degree of internal free volume.[16] It has also been demonstrated that the polyimide incorporating a three-dimensional, rigid triptycene framework has a high internal free volume to allow fast molecular diffusion, thus leading to high gas permeability.[17] To our best knowledge, there are still no reports about the electrosynthesis and electrochromic properties of electroactive poly(amide-triarylamine)s bearing the triptycene moiety. In this study, four diamide derivatives featuring a triptycene as an interior core and terminal electroactive triphenylamine (TPA) or *N*-phenylcarbazole (NPC) groups were prepared, and their electrochemistry and electropolymerization were investigated. The electrochromic properties of the electrogenerated films were evaluated by the spectroelectrochemical and electrochromic switching studies. Incorporation of the three-dimensional,

rigid triptycene unit into the polymer backbones was expected to increase the internal free volume in the polymer film to allow better charge transfer at doping and thus leading to fast switch speeds.

2. Experimental

2.1. Materials

1,4-Bis(4-aminophenoxy)triptycene **(3)** (mp = 254-255 ^{o}C) was synthesized by the aromatic nucleophilic substitution reaction of *p*-chloronitrobenzene with 1,4-dihydroxytriptycene (**1**) in the presence of potassium carbonate, followed by a palladium-catalyzed hydrogen reduction of the intermediate dinitro compound **2** (Scheme 1). The synthetic details and characterization data of triptycene-bis(ether amine) **3** have been described previously.[18] According to the reported procedures,[19] 1,4-bis(4-carboxyphenoxy)triptycene **(5)** (mp = 386-388 ^{o}C) was prepared by the alkaline hydrolysis of 1,4-bis(4-cyanophenoxy)triptycene **(4)** obtained from the fluoro-displacement reaction of *p*-fluorobenzonitrile with 1,4-dihydroxytriptycene in the presence of potassium carbonate. 4-Carboxytriphenylamine **(6)** and *N*-(4-carboxyphenyl)carbazole **(7)** were synthesized by the cesium fluoride (CsF)-mediated *N*-arylation reaction of diphenylamine and carbazole, respectively, with *p*-fluorobenzonitrile, followed by the alkaline hydrolysis of the intermediate dintrile compounds (Scheme 2). According to the reported procedures,[20,21] 4-aminotriphenylamine **(8)** and *N*-(4-aminophenyl)carbazole **(9)** were prepared by the hydrazine Pd/C-catalyzed reduction of 4-nitrotriphenylamine and *N*-(4-nitrophenyl)carbazole, respectively. These two nitro precursors were synthesized from the *N*-arylation of diphenylamine and carbazole, respectively, with *p*-fluoronitrobenzene in the presence of a base. The bis(amide-triarylamine) derivatives **T-TPA-C**, **T-TPA-N**, **T-CBZ-C** and **T-CBZ-N** were prepared by the condensation reactions from 1,4-bis(4-aminophenoxy)triptycene with 4-carboxytriphenylamine and *N*-(4-carboxyphenyl)carbazole, respectively, and from 1,4-bis(4-carboxyphenoxy)triptycene with 4-aminotriphenylamine and *N*-(4-aminophenyl)carbazole, respectively (Scheme 3). The synthetic details and characterization data of these compounds are included in the Supporting Information. Triphenyl phosphite (TPP, Acros) and dichloromethane (Tedia) were used as received. *N*-Methyl-2-pyrrolidone (NMP, Tedia) and pyridine (Py, Wako) were dried over calcium hydride for 24 h, distilled under reduced pressure, and stored over 4 Å molecular sieves in a sealed bottle. Commercially obtained calcium chloride ($CaCl_2$, Wako) was dried under vacuum at 200 ^{o}C for 3 h prior to use. Tetrabutylammonium perchloate, Bu_4NClO_4 (TCI), was recrystallized from ethyl acetate under nitrogen atmosphere and then dried in vacuo prior to use.

2.2. Electrochemical polymerization

Electrochemical polymerization was performed with a CH Instruments 750A electrochemical analyzer. The polymers were synthesized from 10^{-4} M monomers and 0.1 M Bu_4NClO_4 in dichloromethane (CH_2Cl_2)

solution via cyclic voltammetry repetitive cycling at a scan rate of 50 mV s^{-1}. The polymer was deposited onto the surface of the working electrode (ITO/glass surface, polymer films area about 0.7 cm × 3 cm), and the film was rinsed with plenty of acetone for the removal of un-reacted monomer, inorganic salts and other organic impurities formed during the process.

2.3. Instrumentation and measurements

Infrared (IR) spectra were recorded on a Horiba FT-720 FT-IR spectrometer. ^{1}H and ^{13}C NMR spectra were measured on a Bruker AVANCE 500 FT-NMR system with tetramethylsilane as an internal standard. Electrochemical measurements were performed with a CH Instruments 750A electrochemical analyzer. Cyclic voltammetry was conducted with the use of a three-electrode cell in which ITO (polymer film area about 0.8 cm × 1.25 cm) was used as a working electrode. A platinum wire was used as an auxiliary electrode. All cell potentials were taken with the use of a home-made Ag/AgCl, KCl (sat.) reference electrode. Ferrocene was used as an external reference for calibration (+0.48 V vs. Ag/AgCl). Spectroelectrochemistry analyses were carried out with an electrolytic cell, which was composed of a 1 cm cuvette, ITO as a working electrode, a platinum wire as an auxiliary electrode, and a Ag/AgCl reference electrode. Absorption spectra in the spectroelectrochemical experiments were measured with an Agilent 8453 UV-Visible spectrophotometer.

3. Results and discussion

3.1. Monomer synthesis

1,4-Bis(4-aminophenoxy)triptycene (**3**)[18] and 1,4-bis(4-carboxyphenoxy)triptycene (**5**)[19] were synthesized according to the synthetic routes outlined in Scheme 1. The triarylamine derivatives **6–9** used for the end-capping reactions could be easily prepared on the basis of a well-known chemistry (Scheme 2). Four triptycene-cored diamide derivatives end-capped with electroactive TPA or NPC groups were prepared by the condensation reactions from triptycene-bis(ether amine) **3** with 4-carboxytriphenylamine (**6**) and *N*-(4-carboxyphenyl)carbazole (**7**), respectively, and from bis(ether-carboxylic acid) **5** with 4-aminotriphenylamine (**8**) and *N*-(4-aminophenyl)carbazole (**9**), respectively, using TPP and pyridine as condensing agents.[22] As shown in Scheme 3, these four compounds were coded as **T-TPA-C**, **T-CBZ-C**, **T-TPA-N**, **T-CBZ-N**. The former two compounds are isomeric to the latter two ones with different orientations of the amide linkage. The triphenylamine units of compounds **T-TPA-C** and the *N*-phenylcarbazole units of **T-CBZ-C** are attached to the carbonyl side of the amide group, and those of **T-TPA-N** and **T-CBZ-N** are linked to the amide NH side.

The structures of the target compounds were confirmed by means of FTIR spectroscopy and high-resolution NMR analysis. The FTIR spectra of these compounds are included in Fig. S1, where we

can find the characteristic absorption bands of amide group at near 3300 (N–H str.) and 1650 cm^{-1} (amide C=O str.), and the characteristic ether absorption bands at near 1220 cm^{-1} (C–O str.). Figs. S2 to S5 compile the ^{1}H NMR, ^{13}C NMR, H-H COSY, and C-H HSQC spectra of **T-TPA-C**, **T-TPA-N**, **T-CBZ-C** and **T-CBZ-N**, respectively. The assignments of all proton and carbon resonance peaks are also shown in the spectra and they are in good agreement with the proposed molecular structures of these synthesized compounds. The resonance peaks appearing in the downfield regions of the ^{1}H NMR spectra (10−11 ppm) and ^{13}C NMR spectra (164−165 ppm) support the presence of amide groups in the synthesized compounds.

3.2. Electropolymerization

All electrochemical polymerization processes of monomers were performed on the ITO glass slides in a reaction medium containing 10^{-4} M monomer in 0.1 M Bu_4NClO_4/dichloromethane (CH_2Cl_2) solution via repetitive cycling at a potential scan rate of 50 mV s^{-1}. Fig. 1(a) displays the successive cyclic voltammograms (CV) of the **T-TPA-C** solution between 0 and 1.30 V. As the CV scan continued, the **P(T-TPA-C)** polymer film was formed on the working electrode surface. The increase in the redox wave current densities implied that the amount of conducting polymers deposited on the electrode was increasing. The polymerization of **T-TPA-C** showed two oxidation peaks ($E_{1/2}$ = 0.88 and 1.01 V), which are attributed to their polaronic and bipolaronic states, respectively. The inset in Fig. 1(a) displays the first three consecutive CV scans of **T-TPA-C**. In the first scan, only one oxidation peak (E_{pa}) at 1.21 V is observed, which is attributed to the oxidation of TPA. A new oxidation wave appeared as a shoulder at 0.92 V during the second scan, and the wave shifted to a more positive potential with increased current during the third scan. This is a typical oxidation wave of the benzidine group, indicating the occurrence of the oxidative coupling between the TPA units. It has been proposed that the radical cation of TPA dimerizes (couples) or reacts with the parent TPA unit rapidly to form a tetraphenylbenzidine (TPB) segment.[23] The formed dimer TPB is more easily oxidized than the starting TPA unit and undergoes further oxidations in two discrete one-electron steps to the $TPB^{\cdot +}$ monocation and finally the quinoidal TPB^{2+}.

The electrochemical properties of the isomeric **T-TPA-N** are completely different. Fig. 1(b) displays its reversible electrochemical behavior, which indicates that the intermediate produced in the oxidation process of **T-TPA-N** is stable on the time scale of the CV scan. Repetitive scans between 0 and 1.30 V produced almost the same patterns as those observed in the first scan, and no new peaks were detected under these experimental conditions. This reversible process suggests that the radical cation of **T-TPA-N** is more stable than that produced from the oxidation of its **T-TPA-C** isomer. Therefore, no polymer films were built on the electrode surface. The less stability of the **T-TPA-C** radical cation can be explained by the fact that its TPA units are attached to the electron-withdrawing carbonyl side of the amide linkage.

Thus, the orientation of the amide linkage in these compounds significantly affected their electrochemical behaviors and electropolymerization reactions.

Fig. 2(a) presents three consecutive CV scans of **T-CBZ-**C. For the first scan, one oxidation peak (E_{pa}) at 1.82 V due to the oxidation of the CBZ moieties is detected. During subsequent scans, the oxidation peak in the CV is shifted positively with the increasing number of cycles and no polymer films were built on the electrode surface upon repetitive scanning. The electron-withdrawing effect of the carbonyl (C=O) groups led to a relatively higher oxidation potential of the carbazole groups. This might result in an over-oxidation of the compound and undesired side reactions; thus, we could not observe any polymer films were built on the ITO surface. In contrast, the electropolymerization process of the isomeric compound **T-CBZ-N** is feasible. Repeated scans for several cycles at 0-1.60 V led to a thin film built on the electrode, and the resulting **P(T-CBZ-N)** exhibited two reversible redox couples at $E_{1/2}$ values of 0.98 V and 1.30 V. As shown in inset of Fig. 2(b), only one oxidation peak at 1.46 V is observed in the first CV scan of **T-CBZ-N**. After the second scan, a new oxidation peak appeared at 1.03 V that corresponded to the first oxidation of the biscarbazole dimer generated through oxidative coupling of carbazole radical cations.[24] The increase in the redox couples current densities suggests that the amount of electroactive polymers deposited on the electrode is increasing. In comparison to the reversible redox behavior observed for **T-TPA-N**, **T-CBZ-N** revealed a feasible electropolymerization property. This can be attributed to the fact that the planarity of the carbazole system and the attendant high electron density at the reactive sites, the coupling rate of NPCs has been found to be much faster than for the TPAs.[24]

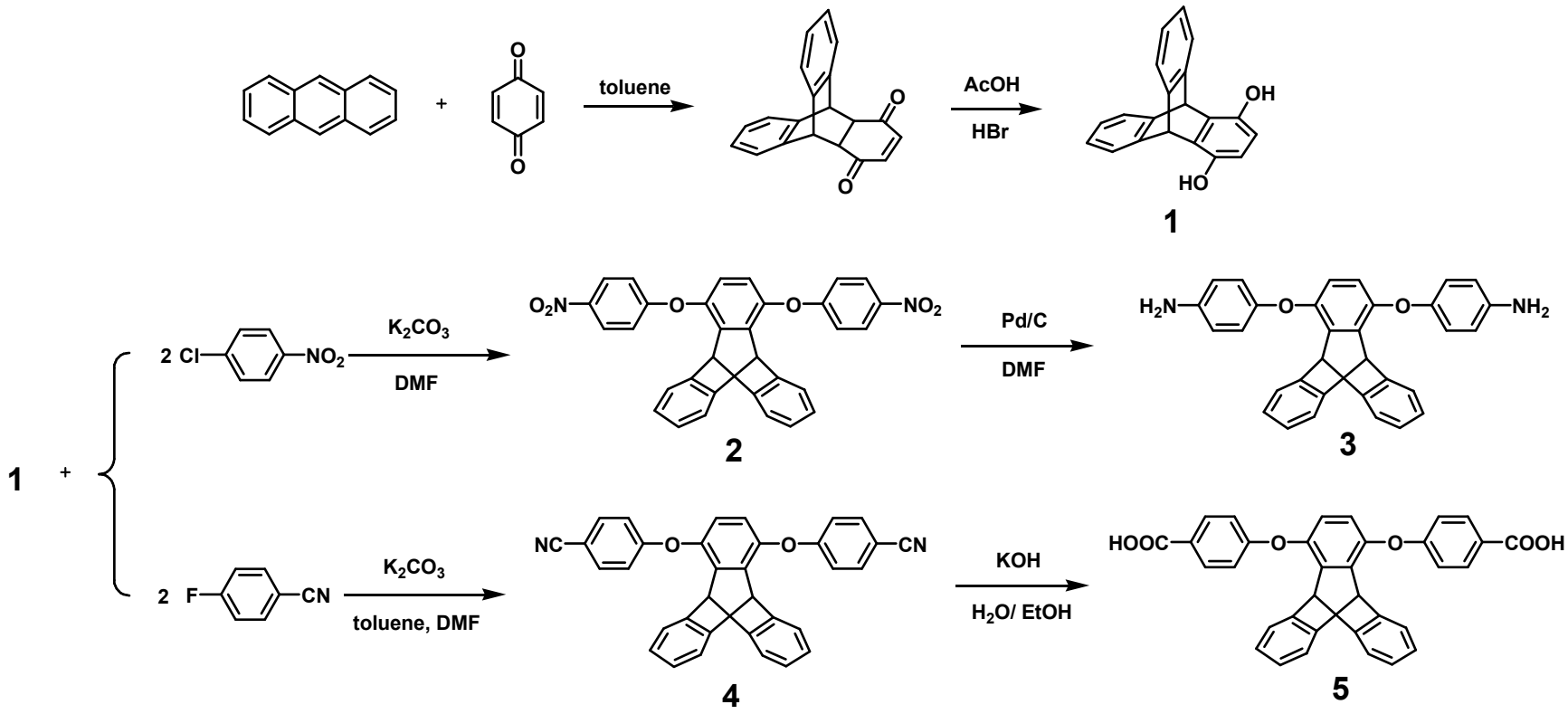

Scheme 1 Synthetic route to triptycene-bis(ether amine) **3** and bis(ether-carboxylic acid) **5**.

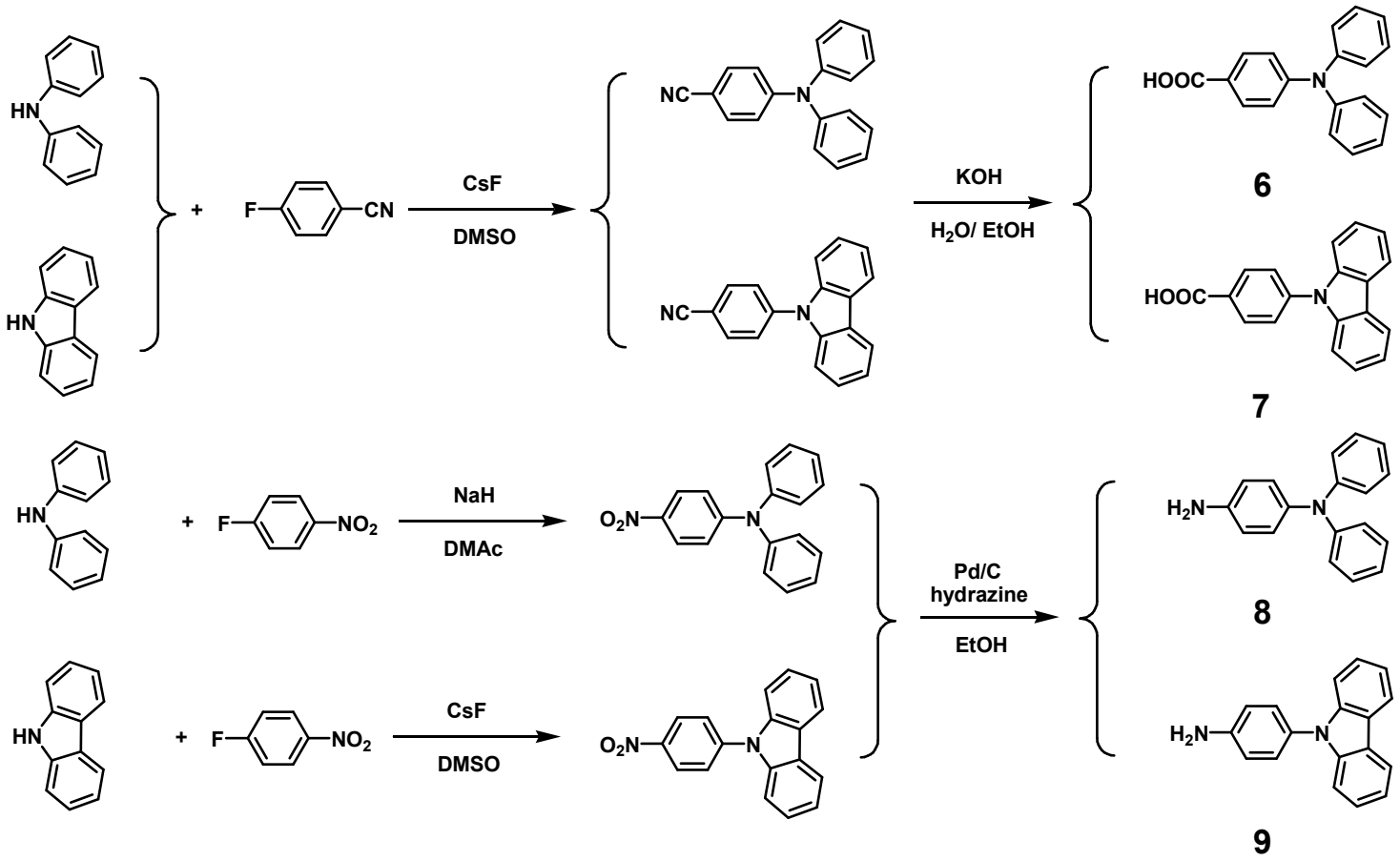

Scheme 2 Synthetic routes to end-capping compounds 4-carboxytriphenylamine **(6)**, *N*-(4-carboxyphenyl)carbazole **(7)**, 4-aminotriphenylamine **(8)**, and *N*-(4-aminophenyl)carbazole **(9)**.

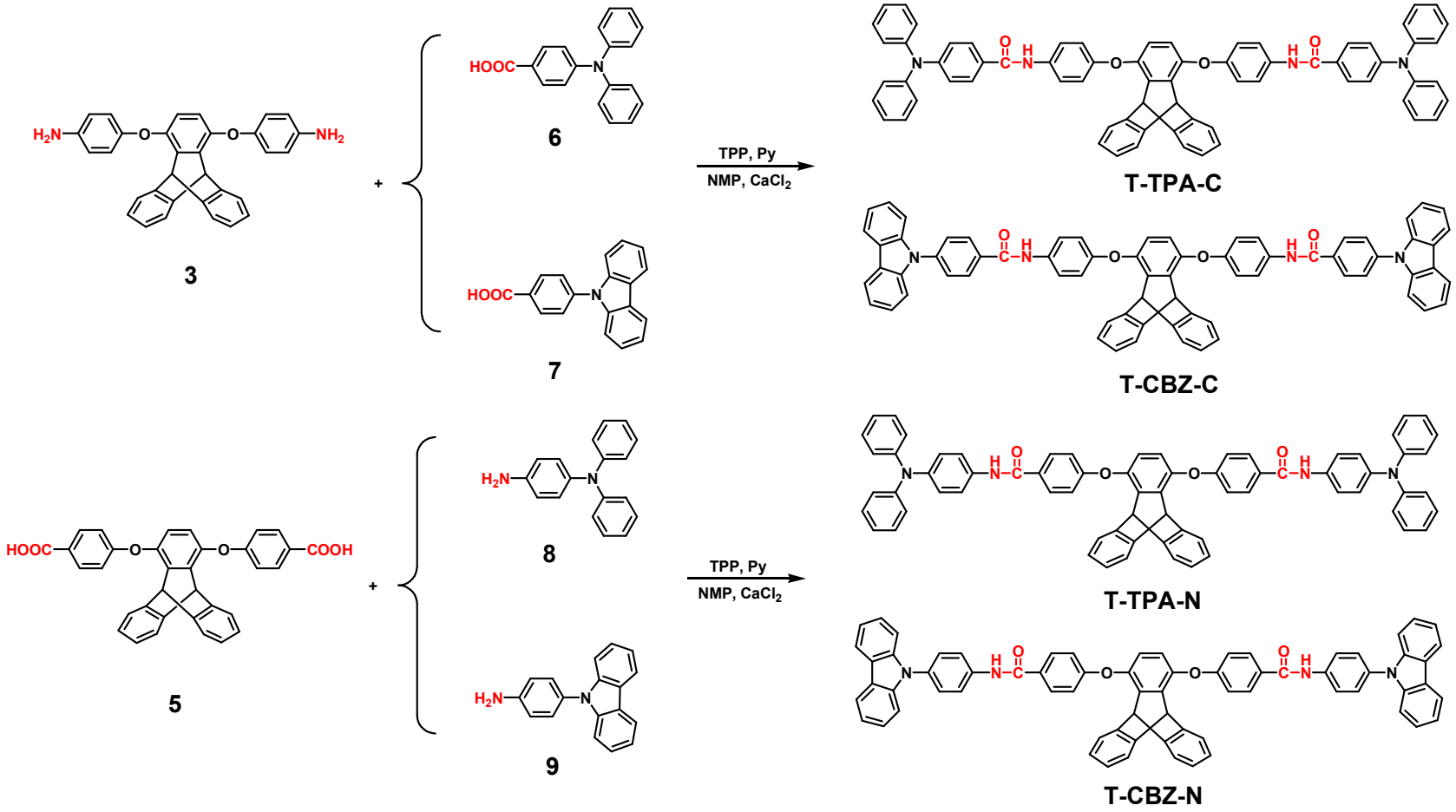

Scheme 3 Synthesis of monomers **T-TPA-C**, **T-CBZ-C**, **T-TPA-N**, and **T-CBZ-N**.

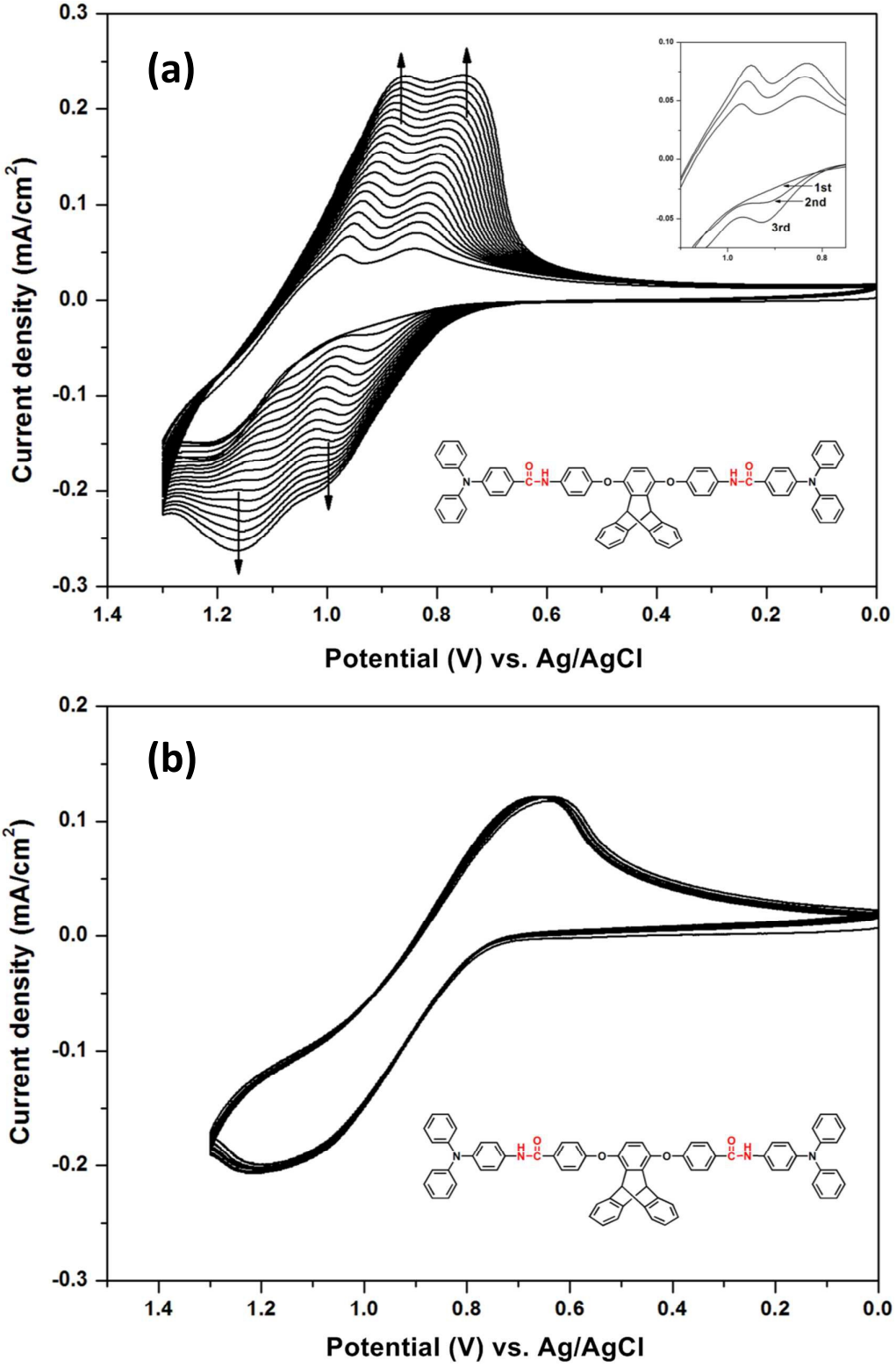

Fig. 1. Repeated potential scanning of (a) **T-TPA-C** and (b) **T-TPA-N** between 0 and 1.30 V in 0.1 M Bu_4NClO_4/CH_2Cl_2 with a scan rate of 50 mV s^{-1}. The inset displays the first, second, and third CV scans of **T-TPA-C**.

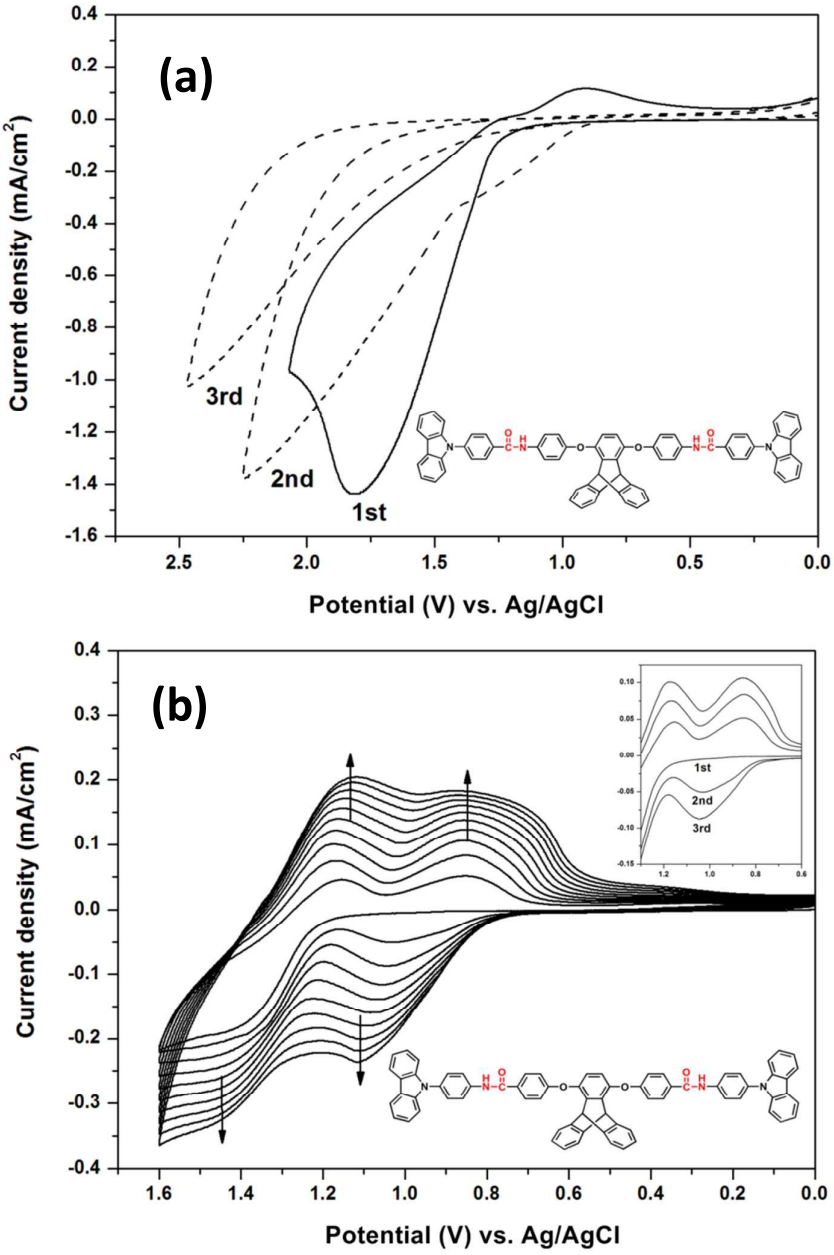

Fig. 2 Repeated potential scanning of (a) **T-CBZ-C** and (b) **T-CBZ-N** monomer in 0.1 M Bu_4NClO_4/CH_2Cl_2 with a scan rate of 50 mV s^{-1}. The inset displays the first, second, and third CV scans of **T-CBZ-N**.

3.3. Electrochemistry of the polymer films

The electrochemical behavior of the electrodeposited polymer films was investigated by cyclic voltammetry in a monomer-free Bu_4NClO_4/CH_3CN solution. Fig. 3(a) and 3(b) respectively displays the CV curves of the **P(T-TPA-C)** and **P(T-CBZ-N)** at different scanning rates between 50 and 300 mV/s. The **P(T-TPA-C)** film shows two closely separated redox couples, one of them centered around 0.93 V and another centered around 1.02 V. The first anodic peak corresponds to one-electron oxidations of the TPB units to form radical cations, followed subsequently by the oxidation to dicationic species (see Scheme 4a). The **P(T-CBZ-N)** film exhibits two reversible redox couples at $E_{1/2}$ value of 1.03 and 1.27 V, attributed to the radical cation and dication states of biscarbazole, respectively (see Scheme 4b). In the scan rate dependence experiments for **P(T-TPA-C)** and **P(T-CBZ-N)** films, both anodic and cathodic peak current values increase linearly with an increasing scan rate (insets of Fig. 3), indicating that the electrochemical processes are reversible and not diffusion limited, and the electroactive polymer is well adhered to the working electrode (ITO glass) surface.

The redox potentials of the investigated polymer films as well as their respective highest occupied molecular orbital (HOMO) and lowest unoccupied molecular orbital (LUMO) (versus vacuum) energy levels are summarized in Table 1. The external ferrocene/ferrocenium (Fc/Fc^+) redox standard has $E_{1/2}$ value of 0.44 V vs Ag/AgCl in acetonitrile. Under the assumption that the HOMO level or called ionization potentials (versus vacuum) for the ferrocene standard was 4.80 eV with respect to the zero vacuum level, the HOMO levels for the electro-generated polymer films are estimated from the $E_{1/2}^{Ox1}$ values of from their CV diagrams as 5.29−5.39 eV. The energy gaps estimated from the absorption spectra were then used to obtain the LUMO energy levels of 2.30−2.35 eV. According to the HOMO and LUMO energy levels obtained, the polymers in this study seem to be appropriate as hole injection and transport materials.

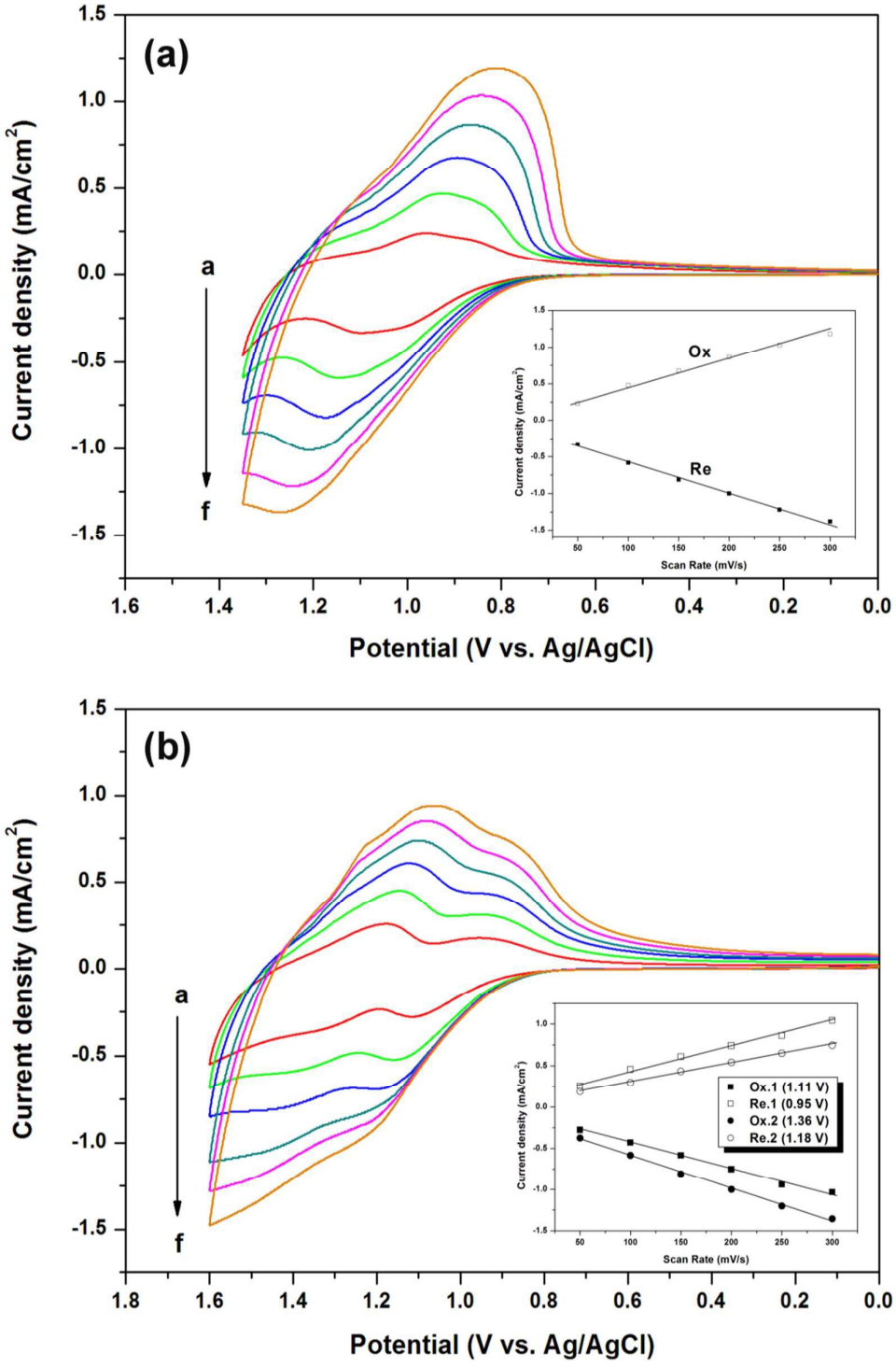

Fig. 3 Scan-rate-dependent cyclic voltammograms of (a) **P(T-TPA-C)** and (b) **P(T-CBZ-N)** in 0.1 M Bu_4NClO_4/CH_3CN solution at different scan rates between 50 and 300 mV/S. (a = 50 mV s^{-1}, b = 100 mV s^{-1}, c = 150 mV s^{-1}, d = 200 mV s^{-1}, e = 250 mV s^{-1} and f = 300 mV s^{-1}). Inset: scan rate dependence of the anodic and cathodic peak current densities graph.

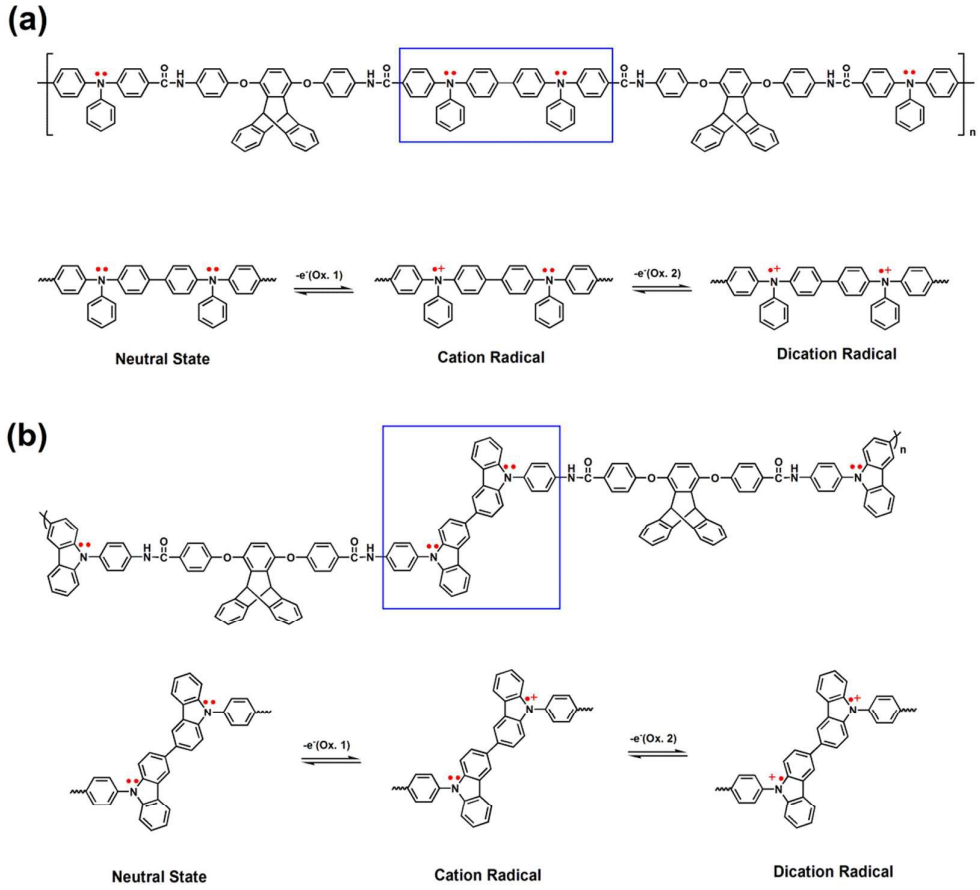

Scheme 4 Anodic oxidation pathways of (a) **P(T-TPA-C)** and (b) **P(T-CBZ-N)**.

3.4. Spectroelectrochemistry and electrochromic switching

The electro-optical properties of the electro-generated polymer films were investigated using the changes in electronic absorption spectra at various applied voltages. Spectroelectrochemical diagrams of th **P(T-TPA-C)** and **P(T-CBZ-N)** polymeric films deposited on ITO were recorded in the monomer-free electrolyte solution. The result of **P(T-TPA-C)** film upon electro-oxidation is presented in Fig. 4(a) as a series of UV-vis-NIR absorption curves correlated to electrode potentials. Before electrical potential was applied, the **P(T-TPA-C)** film showed a strong absorption at 357 nm, but it almost colorless in the visible region. By setting the potential to 1.1 V, the intensity of the absorption band around 357 nm decreased gradually, and the growth of new peaks at 494 and 711 nm was observed. As the potential increased more positively to 1.3 V, the absorbance at 494 nm slightly decreased and the absorption at 711 nm further intensified. Meanwhile, the film changed color from orange to deep blue. We attribute the development of bands at 494 and 711 nm to the formation of TPB radical cations and dications, respectively, as shown in Scheme 4a. The film showed a multicolored electrochromism from colorless neutral state to orange semi-oxidized state and blue fully oxidized state. This phenomenon persisted for several subsequent scans.

Fig. 4(b) shows the spectral changes of the electro-deposited film **P(T-CBZ-N)** upon incremental oxidative scans from 0 to 1.6 V. In the neutral form, at 0.0 V, the **P(T-CBZ-N)** exhibited strong absorption at λ_{max} of 313 nm. As the applied voltage was stepped from 0.0 to 1.2 V, the absorbance at 313 nm decreased, and new peak at 431 nm gradually increased in intensity. In the same time, the film turned into yellowish green. We attribute these spectral changes to the formation of cation radicals of the biscarbazole moieties. At higher oxidation levels (1.2-1.6 V), the absorbance at 431 nm decreased and a new broad absorption band centered at about 859 nm started to intensify and extended into the near-IR region, which indicates the formation of dication states of the polymer film. The inset of Fig. 4(b) shows photographs of the **P(T-CBZ-N)** film in uncharged (neutral, very pale yellow), semi-oxidized (yellowish green) and fully oxidized states (bluish green).

Electrochromic switching studies for the electro-generated poly(amide-triarylamine) films were performed to monitor the percent transmittance changes (ΔT %) as a function of time at their absorption maximum (λ_{max}) and to determine the response time by stepping potential repeatedly between neutral and oxidized states. Fig. 5(a) and 5(b) depict the optical transmittance of **P(T-TPA-C)** film as a function of time at 494 and 711 nm by applying square-wave potential steps between 0 and 1.1 V for a resident time of 6 s and between 0 and 1.3 V for a resident time of 8 s. Generally, the charge passed at 90% of the full optical switch, which was used to evaluate the response time, since the naked eye could not distinguish the color change after this point. As shown in Fig. 5(c), **P(T-TPA-C)** film attained 90% of a complete coloring and bleaching in 1.79 and 0.97 s, respectively. The optical contrast measured as ΔT% between neutral colorless and oxidized orange states was found to be 32 % at 494 nm. Fig. 5(d) shows that **P(T-TPA-C)** attained 90% of a complete coloring and bleaching in 2.92 and 0.99 s, respectively. The

optical contrast measured as Δ*T*% between neutral colorless and oxidized deep blue states was found to be 70 % at 711 nm. The electrochromic coloring efficiency (CE) is defined as the ratio between the change in optical density units and the injected/ejected charge as a function of electrode area (η = $\Delta OD/Q_d$). The CE values of **P(T-TPA-C)** estimated from the data shown in Fig. 5(c) and 5(d) were found to be 348 m^2/C at 494 nm and 151 cm^2/C at 711 nm (Table 1). The fast switch speeds of the polymer film may be attributable to the presence of rigid, three-dimensional framework in the polymer chain which increases the internal free volume in the polymer film to allow rapid counter ion diffusion.

As shown in Fig. 6, **P(T-CBZ-N)** thin film was switched by stepping the potential between 0 and 1.2 V and between 0.0 and 1.6 V for a resident time of 10 s. In this case, a response time required for 90% full-transmittance change of 2.04 s for the coloration step and 1.10 s for the bleaching step at 431 nm, and 2.46 s for the coloration step and 1.42 s for the bleaching step at 859 nm. In addition, the optical contrast measured as Δ*T*% recorded at neutral and oxidized forms was found to be 18 % at 431 nm and 57 % at 859 nm. (Fig. 6(c) and 6(d)). The CE values of **P(T-CBZ-N)** were calculated as 114 m^2/C at 431 nm and 196 cm^2/C at 859 nm (Table 1) by chronoamperometry. The long-term stability of **P(T-CBZ-N)** at yellowish green coloring (λ_{max} = 494 nm) and bluish green coloring (λ_{max} = 711 nm) were investigated by monitoring the electrochromic contrast (Δ*T*%) of the thin film upon repeated square-wave potential steps between 0 and 1.2 V, and between 0 and 1.6V, respectively, as shown in Fig. 6(a) and 6(b). **P(T-CBZ-N)** film still exhibited good reversibility of electrochromic characteristics over 40 cyclic scans between 0 and 1.2 V; however, it showed a remarkably decreased switching stability when stepping between 0 and 1.6 V. The NPC-based polymer film has less long-term switching stability as compared to TPA-based polymer film might be explained by its lower chemical stability during the potential switching.

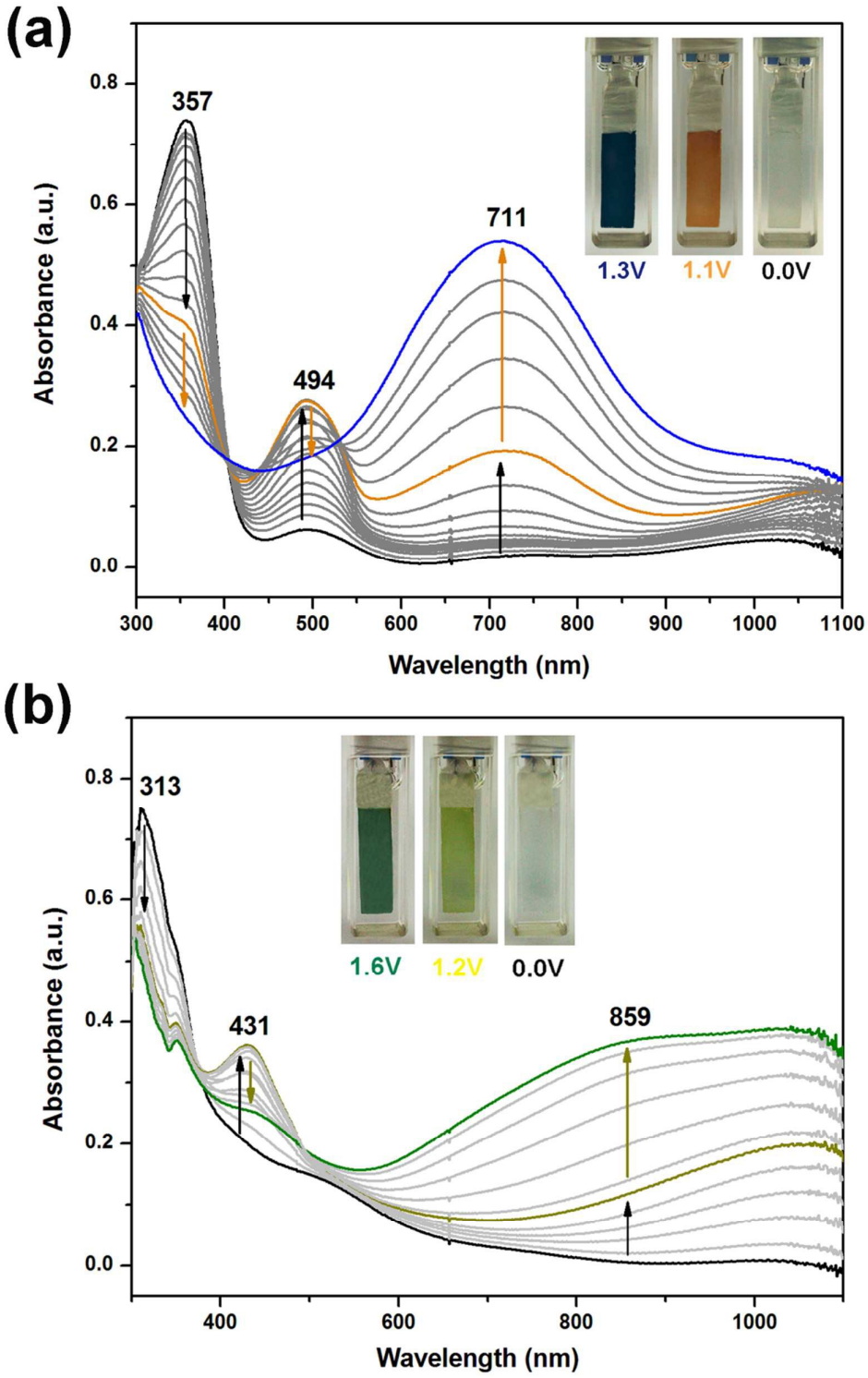

Fig. 4 Spectroelectrograms of (a) **P(T-TPA-C)** and (b) **P(T-CBZ-N)** thin films on the ITO-coated glass substrate in 0.1 M Bu_4NClO_4/CH_3CN solution.

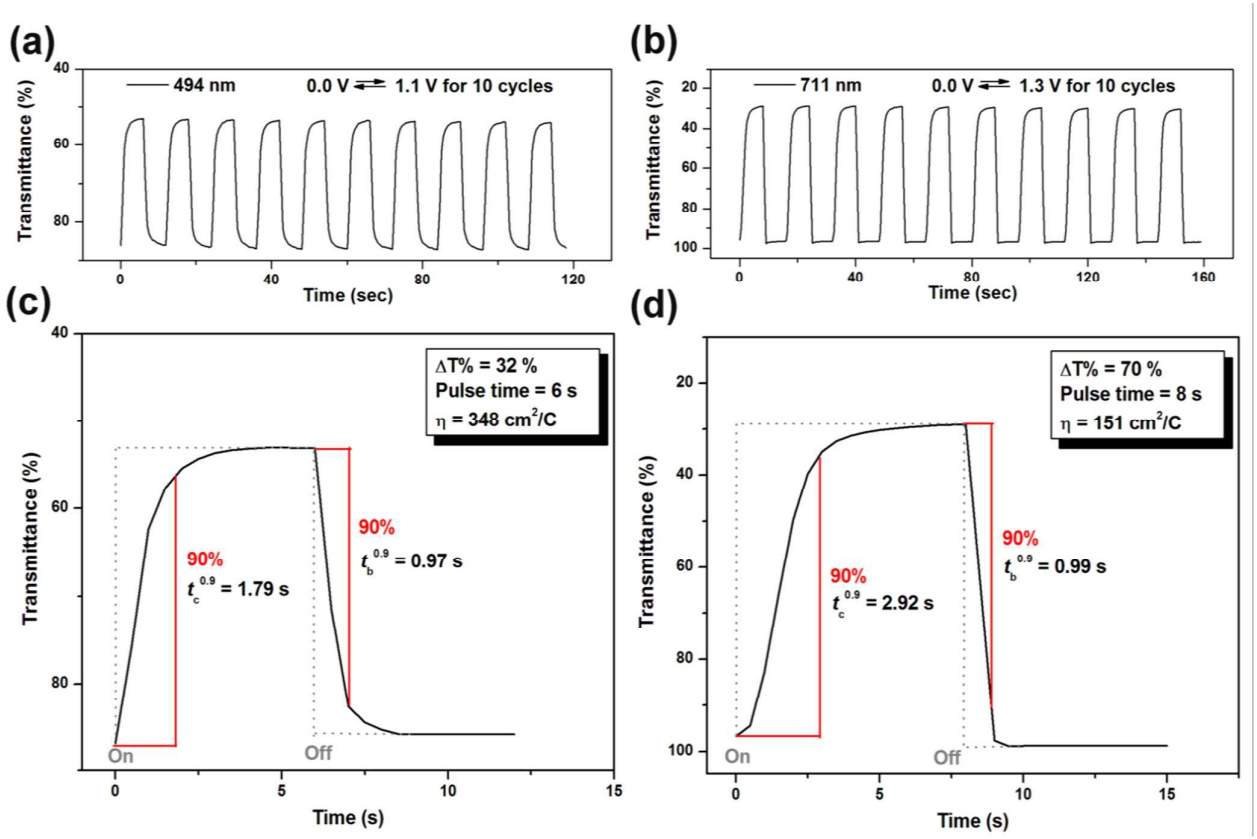

Fig. 5 Potential step absorptometry of the **P(T-TPA-C)** thin film on the ITO-glass slide (in CH_3CN with 0.1 M Bu_4NClO_4 as the supporting electrolyte) by applying a potential step (a) 0.0 V ⇌ 1.1 V with a pulse width of 6 s (b) 0.0 V ⇌ 1.3 V with a pulse width of 8 s. Optical switching at (c) λ_{max} = 494 nm as the applied voltage was stepped between 0 and 1.1 V (vs. Ag/Ag/Cl) and (d) at λ_{max} = 711 nm as the applied voltage was stepped between 0 and 1.3 V (vs. Ag/Ag/Cl).

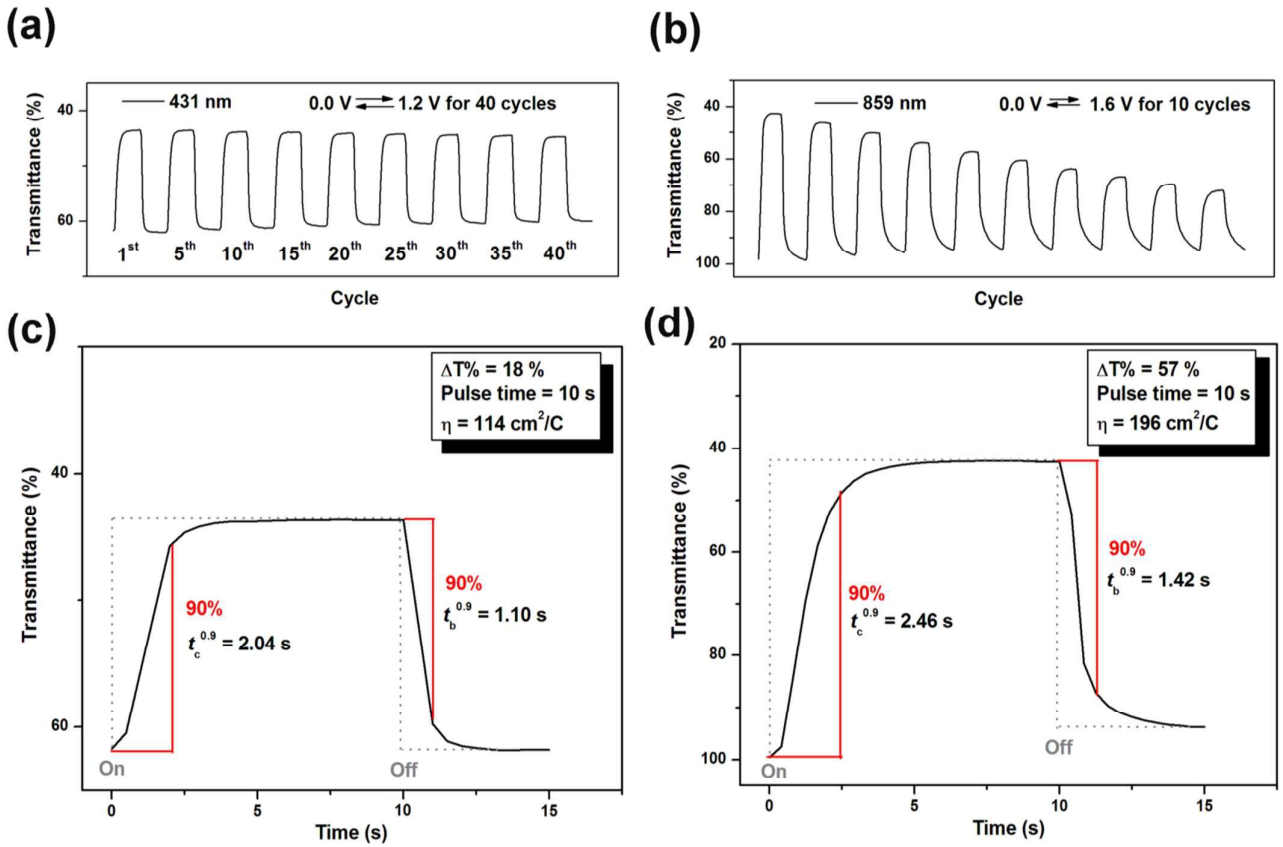

Fig. 6 Potential step absorptometry of the **P(T-CBZ-N)** thin film on the ITO-glass slide (in CH_3CN with 0.1 M Bu_4NClO_4 as the supporting electrolyte) by applying a potential step (a) 0.0 V ⇌ 1.2 V with a switching time of 10 s (b) 0.0 V ⇌ 1.6 V with a switching time of 10 s. Optical switching at (c) λ_{max} = 431 nm as the applied voltage was stepped between 0 and 1.2 V (vs. Ag/Ag/Cl) and (d) at λ_{max} = 859 nm as the applied voltage was stepped between 0 and 1.6 V (vs. Ag/Ag/Cl).

Table 1 Optical, electrochemical and electrochromic data of the electro-generated polymer films

Polymer code	λ_{max}^{abs} (nm)	λ_{onset}^{abs} (nm)	Potential (V) $E_{1/2}^{Ox1}$	Potential (V) $E_{1/2}^{Ox2}$	E_g [a] (eV)	HOMO/ LUMO[b] (eV)	Color of the polymer films[c]	Δ*T*% *(%)*	ΔOD[d]	Q_d[e] (mC cm^{-2})	CE[f] (cm^2 C^{-1})
P(T-TPA-C)	357	415	0.93	1.02	2.99	5.29/2.30	Ox1: Orange	32	0.209	0.60	348
							Ox2: Deep blue	70	0.533	3.53	151
P(T-CBZ-N)	313	408	1.03	1.27	3.04	5.39/2.35	Ox1: Greenish yellow	18	0.151	1.32	114
							Ox2: Bluish green	57	0.371	1.89	196

[a] Bandgaps calculated from the polymer films by the equation: E_g= 1240 /λ_{onset}. [b] The HOMO energy levels were calculated from $E_{1/2}^{Ox1}$ values from the CV diagrams and were referenced to ferrocene (4.8 eV relative to the vacuum energy level, $E_{1/2}^{Ox}$ = 0.44 V vs. Ag/AgCl). $E_{HOMO} = E_{1/2}^{Ox1} + 4.8 - 0.44$ (eV); $E_{LUMO} = E_{HOMO} - E_g$. [c] The colors of polymer films at the partially oxidized state and the fully oxidized state.
[d] Optical Density (ΔOD) = log[$T_{blenched}/T_{colored}$], where $T_{blenched}$ and $T_{colored}$ are the maximum transmittance in the neutral and oxidized states, respectively. [e] Q_d is ejected charge, determined from the *in situ* experiments. [f] Coloration efficiency (CE) =ΔOD/Q_d.

4. Conclusions

Four new triptycene-cotaining bis(amide-triarylamine) compounds **T-TPA-C**, **T-TPA-N**, **T-CBZ-C**, and **T-CBZ-N** derived from 1,4-bis(4-carboxyphenoxy)triptycene or 1,4-bis(4-aminophenoxy)triptycene have been successfully synthesized. Polymer films could be built on the electrode surface from the **T-TPA-C** and **T-CBZ-N** solution by repetitive CV scanning. The electro-deposited films exhibit reversible electrochemical oxidation accompanied by strong color changes having high coloration efficiency that can be switched rapidly through modulation of the applied potential. The **P(T-TPA-C)** film changes color from the almost colorless neutral state to orange and deep blue oxidized states when scanning from 0 to 1.3 V and exhibited good switching stability. The color of **P(T-CBZ-N)** film changes from very pale yellowish neutral form to yellowish green and bluish green oxidized forms upon potential scanning from 0.0 to 1.6 V. The **P(T-CBZ-N)** film shows good switching stability between neutral and first oxidation states; however, it is not so stable at its fully oxidized state. These characteristics suggest that these electro-deposited polymers are promising materials for the use in optoelectronics applications.

Acknowledgement

This work was financially supported by the Ministry of Science and Technology of Taiwan, Republic of China (Grant no. NSC 101-2221-E-027-028-MY3).

Notes and references

1. P. M. S. Monk, R. J. Mortimer and D. R. Rosseinsky, *Electrochromism and electrochromic devices,* Cambridge University Press, Cambridge, UK, 2007.
2. (a) D. R. Rosseinsky and R. J. Montimer, *Adv. Mater.,* 2001, **13**, 783–793; (b) A. Michaelis, H. Berneth, D. Haarer, S. Kostromine, R. Neigl and R. Schmidt, *Adv. Mater.,* 2001, **13**, 1825–1828; (c) H. W. Heuer, R. Wehrmann and S. Kirchmeyer, *Adv. Funct. Mater.,* 2002, **12**, 89–94; (d) G. Sonmez, and H. B. Sonmez, *J. Mater. Chem.,* 2006, **16**, 2473–2477; (e) P. Anderson, R. Forchheimer, P. Tehrani and M. Berggren, *Adv. Funct. Mater.,* 2007, **17**, 3074–3082; (f) R. Baetens, B. P. Jelle and A. Gustavsen, *Sol. Energy Mater. Sol. Cells,* 2010, **94**, 87–105; (g) S. Beaupre, A.-C. Breton, J. Dumas and M. Leclerc, *Chem. Mater.,* 2009, **21**, 1504–1513.
3. (a) A. P. Weidner, U.S. Pat. 7,450,294, 2008; (b) www.gentex.com
4. (a) R. J. Mortimer, *Chem. Soc. Rev.,* 1997, **26**, 147–156; (b) R. J. Mortimer, *Electrochim. Acta,* 1999, **44**, 2971–2981; (c) N. M. Rowley and R. J. Mortimer, *Sci. Prog.,* 2002, **85**, 243–262; (d) R. J. Mortimer, A. L. Dyer and J. R. Reynolds, *Displays*, 2006, **27**, 2–18.
5. (a) S.-H. Baeck, K.-S. Choi, T. F. Jaramillo, G. D. Stucky and E. W. McFarland, *Adv. Mater.,* 2003, **15**, 1269–1273; (b) S.-H. Lee, R. Deshpande, P. A. Parilla, K. M. Jones, B. To, H. Mahan and A. C. Dillon,

Adv. Mater., 2006, **18**, 763–766; (c) G. A. Niklasson and C. G. Granqvist, *J. Mater. Chem.,* 2007, **17**, 127–156.

6. (a) G. Sonmez, *Chem. Commun.,* 2005, 5251–5259; (b) P. M. Beaujuge and J. R. Reynolds, *Chem. Rev.,* 2010, **110**, 268–320; (c) A. Patra and M. Bendikov, *J. Mater. Chem.,* 2010, **20**, 422–433.
7. (a) D. M. Welsh, A. Kumar, M. C. Morvant and J. R. Reynolds, *Synth. Met.,* 1999, **102**, 967–968; (b) L. Groenendaal, F. Jonas, D. Freitag, H. Pielartzik and J. R. Reynolds, *Adv. Mater.,* 2000, **12**, 481–494; (c) L. Groenendaal, G. Zotti, P.-H. Aubert, S. M. Waybright and J. R. Reynolds, *Adv. Mater.*, 2003, **15**, 855–879; (d) A. A. Argun, P.-H. Aubert, B. C. Thompson, I. Schwendeman, C. L. Gaupp, J. Hwang, N. J. Pinto, D. B. Tanner, A. G. MacDiarmid and J. R. Reynolds, *Chem. Mater.,* 2004, **16**, 4401–4412.
8. (a) P. Schottland, K. Zong, C. L. Gaupp, B. C. Thompson, C. A. Thomas, I. Giurgiu, R. Hickman, K. A. Abboud and J. R. Reynolds, *Macromolecules,* 2000, **33**, 7051–7061; (b) K. Zong and J. R. Reynolds, *J. Org. Chem.,* 2001, **66**, 6873–6882; (c) G. Sonmez, I. Schwendeman, P. Schottland, K. Zong and J. R. Reynolds, *Macromolecules,* 2003, **36**, 639–647; (d) R. M. Walczak and J. R. Reynolds, *Adv. Mater.*, 2006, **18**, 1121–1131; (e) R. M. Walczak, J.-H. Jung, J. S. Cowart, Jr. and J. R. Reynolds, *Macromolecules,* 2007, **40**, 7777–7785.
9. (a) G. E. Gunbas, A. Durmas and L. Toppare, *Adv. Mater.,* 2008, **20**, 691–695; (d) G. E. Gunbas, A. Durmus and L. Toppare, *Adv. Funct. Mater.,* 2008, **18**, 2026–2030; (c) A. Balan, D. Baran and L. Toppare, *Polym. Chem.,* 2011, **2**, 1029-1043; (d) A. Cihaner and F. Algi, *Adv. Funct. Mater.,* 2008, **18**, 3583–3589; (e) M. Icli, M. Pamuk, F. Algi, A. M. Onal and A. Cihaner, *Chem. Mater.,* 2010, **22**, 4034–4044; (f) M. I. Ozkut, S. Atak, A. M. Onal and A. Cihaner, *J. Mater. Chem.,* 2011, **21**, 5268–5272; (g) F. Baycan Koyuncu, E. Sefer, S. Koyuncu and E. Ozdemir, *Macromolecules* 2011, **44**, 8407–8414; (h) E. Karabiyik, E. Sefer, F. Baycan Koyuncu, M Tonga, E. Ozdemir and S. Koyuncu, *Macromolecules*, 2014, **47**, 8575–8584.
10. (a) M. Thelakkat, *Macromol. Mater. Eng.,* 2002, **287**, 442–461; (b) Y. Shirota and H. Kageyama, *Chem. Rev.,* 2007, **107**, 953–1010. (c) P.-L. T. Boudreault, S. Beaupre and M. Leclerc, *Polym. Chem.,* 2010, **1**, 127–136; (d) C.-C. Lee, M.-k. Leung, P.-Y. Lee, T.-L. Chiu, J.-H. Lee, C. Liu and P.-T. Chou, *Macromolecules,* 2012, **45**, 751–765.
11. H.-J. Yen and G.-S. Liou, *Polym. Chem.,* 2012, **3**, 255–264.
12. (a) G.-S. Liou and C.-W. Chang, *Macromolecules*, 2008, **41**, 1667–1674; (b) C.-W. Chang and G.-S. Liou, *J. Mater. Chem*., 2008, **18**, 5638–5646; (c) G.-S. Liou and H.-Y. Lin, *Macromolecules*, 2009, **42**, 125–134; (d) H.-J. Yen and G.-S. Liou, *Chem. Mater*., 2009, **21**, 4062–4070; (e) H.-J. Yen, H.-Y. Lin and G.-S. Liou, *Chem. Mater.,* 2011, **23**, 1874–1882; (f) J.-H. Wu and G.-S. Liou, *Adv. Funct. Mater*., 2014, **24**, 6422–6429.
13. (a) Y.-C. Kung and S.-H. Hsiao, *J. Mater. Chem.,* 2010, **20**, 5481–5492; (b) Y.-C. Kung and S.-H. Hsiao, *J. Mater. Chem.,* 2011, **21**, 1746–1754; (c) S.-H. Hsiao, H.-M. Wang, P.-C. Chang, Y.-R. Kung and T.-M. Lee, *J. Polym. Sci. A: Polym. Chem*., 2013, **51**, 2925–2938; (d) H.-M. Wang and S.-H. Hsiao, *J. Polym.*

Sci. A: Polym. Chem., 2014, **52**, 272–286; (e) H.-M. Wang and S.-H. Hsiao, *J. Mater. Chem. C,* 2014, **2**, 1553–1564; (f) S.-H. Hsiao, H.-M. Wang and S.-H. Liao, *Polym. Chem*., 2014, **5**, 2473–2483.

14. (a) X. Jia, D. Chao, H. Liu, L. He, T. Zheng, X. Bian and C. Wang, *Polym. Chem*., 2011, **2**, 1300−1306; (b) H. Niu, H. Kang, J. Cai, C. Wang, X. Bai and W. Wang, *Polym. Chem*., 2011, **2**, 2804−2817; (c) L. Ma, H. Niu, J. Cai, P. Zhao, C. Wang, Y. Lian, X. Bai and W. Wang, *J. Mater. Chem. C*, 2014, **2**, 2272−2282; (d) Y. Wang, Y. Liang, J. Zhu, X. Bai, X. Jiang, Q. Zhang and H. Niu, *RSC Adv*., 2015, **5**, 11071−11076.
15. (a) M.-Y. Chou, M.-k. Leung, Y. O. Su, C.-L. Chiang, C.-C. Lin, J.-H. Liu, C.-K. Kuo and C.-Y. Mou, *Chem. Mater.*, 2004, **16**, 654–661; (b) J. Natera, L. Otero, L. Sereno, F. Fungo, N.-S. Wang, Y.-M. Tsai, T.-Y. Hwu and K.-T. Wong, *Macromolecules*, 2007, **40**, 4456–4463; (c) J. Natera, L. Otero, F. D'Eramo, L. Sereno, F. Fungo, N.-S. Wang, Y.-M. Tsai and K.-T. Wong, *Macromolecules*, 2009, **42**, 626–635; (d) O. Usluer, S. Koyuncu, S. Demic and R. A. J. Janssen, *J. Polym. Sci. B: Polym. Phys*., 2011, **49**, 333–341; (e) S.-H. Hsiao and J.-W. Lin, *Macromol. Chem. Phys*., 2014, **215**, 1525–1532; (f) S.-H. Hsiao and J.-W. Lin, *Polym. Chem.*, 2014, **5**, 6770–6778.
16. T. M. Long and T. M. Swager, *J. Am. Chem. Soc*., 2003, **125**, 14113–14119.
17. Y. J. Cho and H. B. Park, *Macromol. Rapid Commun*., 2011, **32**, 579–586.
18. S.-H. Hsiao, H.-M. Wang, W.-J. Chen, T.-M. Lee and C.-M. Leu, *J. Polym. Sci. A: Polym. Chem*., 2011, **49**, 3109–3120.
19. S.-H. Hsiao, H.-M. Wang, J.-S. Chou, W. Guo and T.-H. Tsai, *J. Polym. Res.,* 2012, **19**:9902 (10 pages).
20. W.-Y. Lee, T. Kurosawa, S.-T. Lin, T. Higashihara, M. Ueda and W.-C. Chen, *Chem. Mater.,* 2011, **23**, 4487–4497.
21. G.-S. Liou, S.-H. Hsiao, N.-K. Huang and Y.-L. Yang, *Macromolecules*, 2006, **39**, 5337–5346.
22. N. Yamazaki, M. Matsumoto and F. Higashi, *J. Polym. Sci. Polym. Chem. Ed*., 1975, **13**, 1373–1380.
23. (a) E. T. Seo, R. F. Nelson, J. M. Fritsch, L. S. Marcoux, D. W. Leedy and R. N. Adams, *J. Am. Chem. Soc.*, 1966, **88**, 3498−3503; (b) R. F. Nelson and R. N. Adams, *J. Am. Chem. Soc.,* 1968, **90**, 3925−3930; (c) S. C. Creason, J. Wheeler and R. F. Nelson, *J. Org. Chem.,* 1972, **37**, 4440−4446.
24. (a) J. F. Ambrose and R. F. Nelson, *J. Electrochem. Soc.*, 1968, **115**, 1159−1164; (b) J. F. Ambrose, L. L. Carpenter and R. F. Nelson, *J. Electrochem. Soc.*, 1975, **122**, 876−894.